How Does Influenza Virus A Escape from Amantadine?

Guangrong Qin,[†] Kunqian Yu,*[,†] Ting Shi,[†] Cheng Luo,[†] Guohui Li,[‡] Weiliang Zhu,[†,§] and Hualiang Jiang*[,†,§]

Drug Discovery and Design Center, State Key Laboratory of Drug Research, Shanghai Institute of Materia Medica, Chinese Academy of Sciences, Shanghai 201203, China, School of Pharmacy, East China University of Science and Technology, Shanghai 200237, China, and Laboratory of Molecular Modeling and Design, State Key Laboratory of Molecular Reaction Dynamics, Dalian Institute of Chemical Physics, Chinese Academy of Sciences, 116023, China

Received: December 7, 2009; Revised Manuscript Received: May 6, 2010

Antiflu drugs such as amantadine (AMT) were reported to be insensitive to influenza A virus gradually after their marketing. Mutation experiments indicate that the trans-membrane domain of M2 protein plays an essential role in AMT resistance, especially the S31N mutation. To investigate the details of structure and mechanism, molecular dynamics (MD) simulations and quantum mechanics/molecular mechanics (QM/MM) calculations have been carried out on both the wild-type protein and its S31N mutant. Our MD simulations reveal AMT can occupy different binding positions in the pore of M2 channel, and the binding modes have also been verified and analyzed by QM/MM calculations. More importantly, we find the formation of a water wire modulated by the binding position of AMT to be essential for the function of M2 protein, and, the block of water wire can inhibit channel function in the WT system. Failure of channel blocking would cause AMT drug resistance in the S31N mutant. These results support one of the conflicting views about M2−drug binding sites: AMT binds to the pore of M2 channel. Our findings help clarify the resistant mechanism of AMT to M2 protein and should facilitate the discovery of new drugs for treating influenza A virus.

Introduction

Influenza A virus has caused several worldwide epidemics, greatly threatening human beings.[1] It consists of three major subviral components, namely, the core, the envelope and the bridge between core and envelope. On the envelope of the viral particle, there are two glycoproteins (hemagglutinin, neuraminidase) and a membrane matrix protein M2.[2] Hemagglutinin binds to the host cell surface sialic acid receptor and initiates virus infection. After virus replication, neuraminidase removes sialic acid from the interface between virus and cellular glycoprotein to facilitate the release of the virus and its spreading to new cells.[3] Compared to neuraminidase and hemagglutinin, M2 protein is more conserved and it plays a key role in virion replication. It equilibrates pH across the viral membrane during entry and across the trans-Golgi membrane of infected cells during viral maturation.[4]

Historically, four drugs were developed to fight against influenza A virus, namely, amantadine, rimantadine (a derivative of amantadine), oseltamivir and zanamivir. The latter two drugs were designed against neuraminidase, and they are still effective for targeting current viruses.[5] Amantadine and rimantadine were designed against M2 protein. However, after its approval for treatment of influenza A, resistance gradually increased. By 2006, almost 100% of H3N2 subtype of avian influenza viruses became AMT resistant in some Asian countries, and 15.5% of H1N1 viruses, which are now prevalent worldwide, are resistant to AMT. Why did AMT and rimantadine become resistant to influenza A virus?

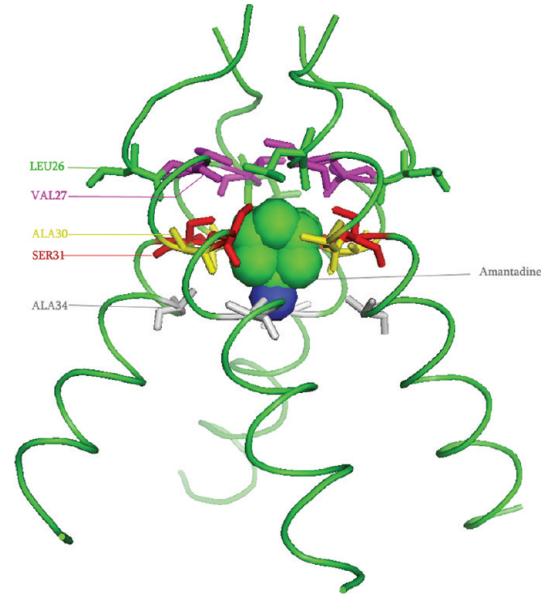

Figure 1. The structure of M2 and amantadine resisting residues. AMT is displayed in CPK; residues whose mutations lead to drug resistance are displayed in colored sticks.

Mutation experiments have been carried out by Suzuki et al. to investigate the AMT resistance. Single point mutations are performed at positions 26, 27, 30, 31 and 34, which are located in the trans-membrane domain of M2 channel [Figure 1].[6] Statistical data shows that in resistant mutants, 70% to 80% of substitutions occur at position 31, and around 10% occur at positions 27 and 30 in vitro and in clinical samples.[6] Moreover,

* To whom correspondence should be addressed. E-mail: kqyu@mail.shcnc.ac.cn or hljiang@mail.shcnc.ac.cn. Phone: +86-21-50806600. Fax: +86-21-50807088.
[†] Shanghai Institute of Materia Medica, Chinese Academy of Sciences.
[‡] Dalian Institute of Chemical Physics, Chinese Academy of Sciences.
[§] East China University of Science and Technology.

10.1021/jp911588y
Published on Web 06/03/2010

TABLE 1: Simulation Systems[a]

system	WT	WT-Lig	WT-H	WT-Lig-H	S31N	S31N-Lig	S31N-H	S31N-Lig-H
residue 31	SER	SER	SER	SER	ASN	ASN	ASN	ASN
residue 37	HISB	HISB	HISH	HISH	HISB	HISB	HISH	HISH

[a] HISB represents H on NE2 only; HISH represents H on ND1 and NE2.

it is indicated that AMT affects the function of the M2 proton channel mainly by changing the distribution and exchange rate among multiple low-energy conformations, and AMT binding only induces subtle variation in the conformation and orientation of M2 protein. Thus AMT-resistant mutations may arise from binding-incompetent changes in the conformational equilibrium.[7] Electrophysiological measurements show that drug-resistant mutations have minimal effects on M2's function and suggest that resistance could be achieved by altering a binding site within the pore rather than a less direct allosteric mechanism.[8]

Based on the mentioned experimental results, two model systems with different binding sites of AMT to M2 had been proposed. One structure of M2 resolved by X-ray scattering technique (PDB name: 3C9J) showed that AMT blocked the channel in the pore, which is quite near serine at position 31.[9] The other structure of M2 complexed with rimantadine was determined using solution NMR (PDB name: 2RLF), which indicates that rimantadine binds to M2 between two neighboring chains facing the lipid side.[10] The two binding patterns suggest different drug inhibiting mechanisms. The former binding pattern holds that AMT directly blocks the channel and therefore the transmission of protons is disrupted. The latter considers that drug binds at four equivalent sites near the tryptophan gate on the lipid-facing side of the channel and stabilizes the closed conformation of the pore.[10] Each theory was supported by some evidences. Jing et al. indicated that AMT bound to the pore of the M2 channel of influenza A virus from their functional studies.[11] On the contrary, Pielak et al. found that replacement of Asp44 with Ala had a dramatic effect on drug sensitivity, but the channel remains fully drug sensitive after replacing Ser31 with Ala.[4] However, the mechanism of the AMT resistance is still unclear.

To better understand the drug inhibiting and resisting mechanism, molecular dynamics (MD) simulations and quantum mechanics/molecular mechanics (QM/MM) calculations were performed in this work. Structures of both wild-type and S31N mutation with AMT binding to the different positions in the pore of M2 channel were obtained, and the binding modes, hydrogen bond modes and water penetrating abilities were characterized. Hydrophobic features and steric hindrance effects were also analyzed in detail for both wild-type and S31N mutation systems. Our results indicate that the formation of a water wire, which is modulated by the binding position of AMT, is essential for the function of M2 protein. This conclusion is in good agreement with the blocking theory and beneficial to understanding the resistant mechanism of AMT to M2 protein.

Materials and Methods

System Preparation. The crystallographic coordinates of trans-membrane domain of M2 protein complexed with AMT extracted from the Protein Data Bank (PDB entry: 3C9J[9]) were used as the initial structure for molecular dynamics simulations. Eight systems were set up and designated as WT, WT-Lig, WT-H, WT-Lig-H, S31N, S31N-Lig, S31N-H, S31N-Lig-H (Table 1). The S31N mutant was derived from mutation at position 31 from Ser to Asn using Sybyl 6.8 package (TRIPOS Inc., 1699 South Hanley Rd., St. Louis, MO 63144). For both WT and S31N system there were no ligands in the systems. The crystal structure 3C9J with AMT was named as WT-Lig in our simulation. To get the same initial position of AMT, both WT and S31N protein were aligned, and then the coordinates of AMT in WT system were copied to the S31N system. WT-H, WT-Lig-H, S31N-H, and S31N-Lig-H were the HIS37 protonated states of WT, WT-Lig, S31N, S31N-Lig, respectively.

Molecular Dynamics Simulation. All MD simulations were carried out using GROMACS 4.0.5 package[12] and an identical protocol. All systems were embedded in DOPC lipid bilayer.[13] GRASP was used to generate solvent-accessible protein surface. Bad contacts of the lipid inside the surface of protein were removed.[33] The mdrun_hole program was used to drive the lipids out of the protein surface.[34,35] Waters were added at a density of 1 g/mL in a cubic periodic box, which was 66 Å × 65 Å × 74 Å. Sodium ions were added to maintain charge neutrality. The GROMOS96 53a6 force field was applied to the protein, lipid parameters adapted from previous MD studies of lipid bilayers.[13] The partial charge of AMT was calculated by Gaussian03 (HF/6-311G**), and other parameters for AMT were calculated by PRODRG, using the GROMOS96 force field.[14] All covalent bonds to hydrogen atoms were constrained using the linear constraint solver (LINCS) method. Electrostatic interactions were calculated using the particle-mesh Ewald (PME) algorithm. Periodic boundary conditions were applied to avoid edge effects in all calculations. Before the MD run, the energy of these complexes was minimized to remove conflicting contacts. Then the systems were heated gradually from 0 to 310 K. After a 300 ps equilibration of water, the lipids were equilibrated for 10 ns with the protein and AMT restrained to reduce the influence of lipid on the protein. Then, two 300 ps equilibrations of the system were carried out with the restriction of main chain and carbon α helix respectively. Finally, 30 ns simulations were carried out, with coordinates saved every 1 ps during the entire process. The eight systems were simulated for three times in parallel.

Clustering Analysis. In order to find representative conformations from the saved trajectories, root-mean-square deviation (rmsd)-based conformational clustering analysis was performed using GROMACS (g_cluster). Structures were extracted every 10 ps over each simulation. 3000 structures for each simulation were superimposed using α carbon (CA) atoms. A rmsd cutoff of 0.11 nm was chosen as the criterion to assign a cluster.

QM/MM Calculations. Using the same initial structures of WT and S31N mutation in MD simulations as the starting conformations, AMT was put into different positions of the channels according to the binding positions in the WT binding site (near SER31, between S31N and ALA34) and S31N binding site (near HIS37, between HIS37 and ALA34) in MD simulations, forming four systems, WT-AMT, S31N-AMT, WT-AMT′ and S31N-AMT′. The binding energies of the four structures were obtained using the QM/MM approach. AMT and M2 proteins (including WT and S31N mutation) were optimized respectively. The QM region is composed of Ser31 (Asn31), Ala30 and AMT, while the rest of system was regarded as the MM region. ONIOM[15−19] (B3LYP/6-31G:Amber), a QM/MM

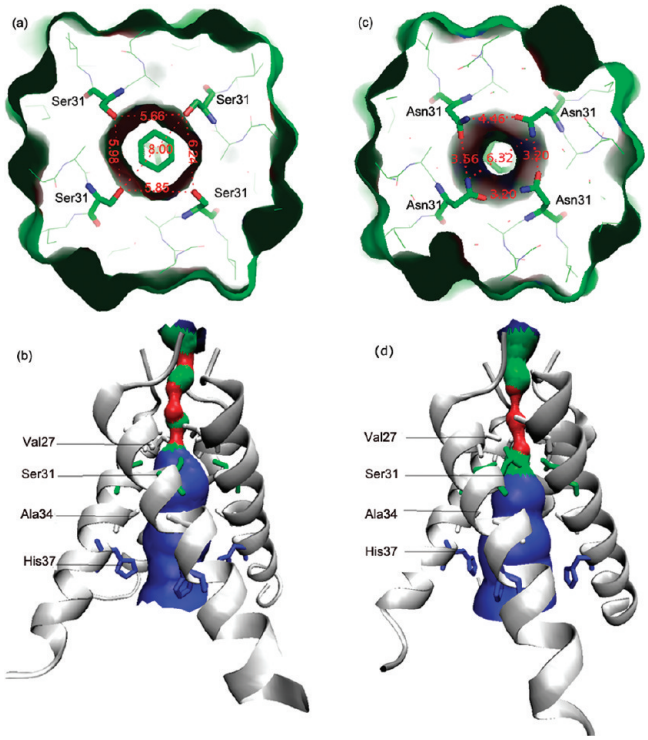

Figure 2. An illustration of the pore size of wild type M2 protein and S31N mutation. (a) Top view of WT M2 channel; the outer surface and inner surface of the channel are represented, and AMT is located in the pore. (b) Side view of WT M2 channel; residues near the surface of M2 channel are shown in sticks, and the pore radii are shown in different colors. Red: inaccessible to water (pore radius < 1.15 Å). Green: water accessible parts (1.15 Å < pore radius < 2.3 Å). Blue: wide areas (pore radius > 2.3 Å). (c) Top view of S31N M2 channel. (d) Side view of S31N M2 channel.

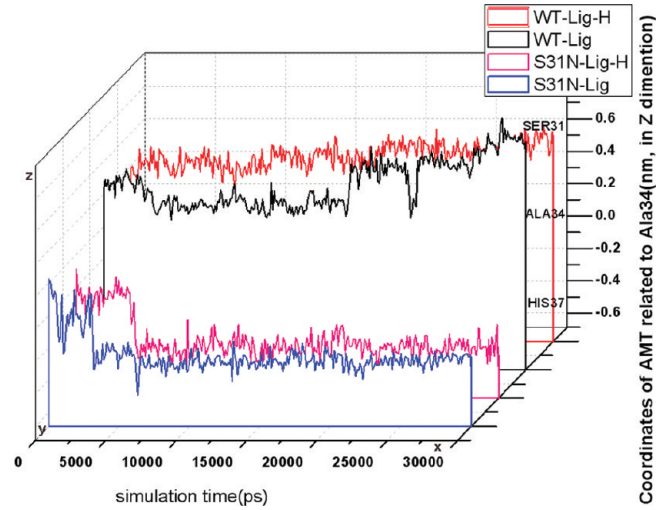

Figure 3. Drug binds to different position in the pore of M2. The distance in *Z* dimension between amantadine and the center coordinate of Ala34 from each chain. The *X* axis is the MD simulation time. The *Z* axis has two scales: one is the relative coordinate; the other is the relative position of residues in M2 protein.

method encoded in Gaussion03,[20] was used for all the QM/MM calculations.

Results and Discussion

AMT Binds to Different Sites in Wild Type and Drug Resistant System. It is reported that influenza A virus has developed two alternate routes to avoid blocking its channel: (1) the channel no longer binds the blocker and hence the blocker cannot exert its inhibitory function; (2) binding of the blocker is retained, yet the function of the protein is unaffected.[21] To study the drug resistance mechanism for the M2 protein channel, eight simulation systems including WT, WT-Lig, WT-H, WT-Lig-H, S31N, S31N-Lig, S31N-H, S31N-Lig-H (see Materials and Methods for details) were used to investigate the dynamics of these systems. After energy minimization and equilibration, 30 nanoseconds (ns) of MD simulations were obtained. The RMSD values for each system show that all reach equilibrium (see Figure S1 in Supporting Information), which provides a solid foundation for further analysis.

Using the Hole program,[22] we can see that the trans-membrane domain of M2 has formed "gates" at four narrow points, namely, positions Val27, Ala34, His37 and Trp41. The latter two residues are recognized as the pH sensor and gate of M2, and Val27 was indicated as a second gate of M2.[23,24] For the WT M2 protein, the hole diameter made from four Ser31 of separate trans-membrane chains is about 8 Å [Figure 2a]. However, after the mutation of residue 31 from Ser to Asn, the diameter for this hole was reduced to 6.32 Å [Figure 2b]. The X-ray structure of M2−AMT complex shows that AMT is located in the hole between Ser31 and Ala34 [Figure 1]. AMT is a very rigid molecule, and the largest distance between any two atoms in AMT is about 5 Å. With the mutation of Ser31 to Asn, the side chain at that position is changed from $-CH_2OH$ to $-CH_2CONH_2$, leaving less space for AMT entering or being stabilized.

The initial positions of AMT in WT-Lig and S31N-Lig system were assigned to be located between Ser31 and Ala34 as described in Materials and Methods. During the 30 ns simulations, AMT moved to different positions in the M2 channel. In both the WT-Lig and WT-Lig-H systems, AMT remains stable near the crystal structure position. However, in the S31N-Lig and S31N- Lig-H systems, AMT can no longer stay in that position. As Figure 3 shows, the binding position of AMT is influenced by the residue in position 31. The binding sites of AMT show a significant difference between WT and S31N systems. However, little difference is shown between the different protonation states of histidine. We calculated the distances between AMT and Ala34 for the whole trajectories in the *Z* dimension, which is along the channel in WT-Lig and S31N-Lig systems [Figure S2 in the Supporting Information]. As shown in Figure 3, the coordinates of AMT related to Ala34 range from 0.7 to 0.3 nm in the WT-Lig system, and most of the relative coordinates clustered near 0.4 nm. In contrast, the coordinates of AMT related to Ala34 in the S31N-Lig system range from 0.2 nm to −0.5 nm, and there is a cluster near −0.4 nm [Figure 3]. Here a positive real number means near the N-terminal, and a negative number means near the C-terminal. The distance between dominant binding positions of AMT to the channel for WT and S31N system is about 8 Å during the simulation [Figure 3]. The different stable binding sites in each system indicate that the protein−drug interaction modes between the WT and S31N systems are different, which may lead to drug resistance.

Mechanism of AMT Binding and Drug Resisting. Cluster Analysis Shows the Steric Hindrance Is One Reason for Different Drug Binding Modes. The 30 ns simulations of those eight systems (WT, WT-H, S31N, S31N-H, WT-Lig, WT-Lig-H, S31N-Lig, S31N-Lig-H) produced 8 × 30000 conformations. To get representative conformations, we used a tool (g_cluster) in GROMACS to analyze all those conformations based on the

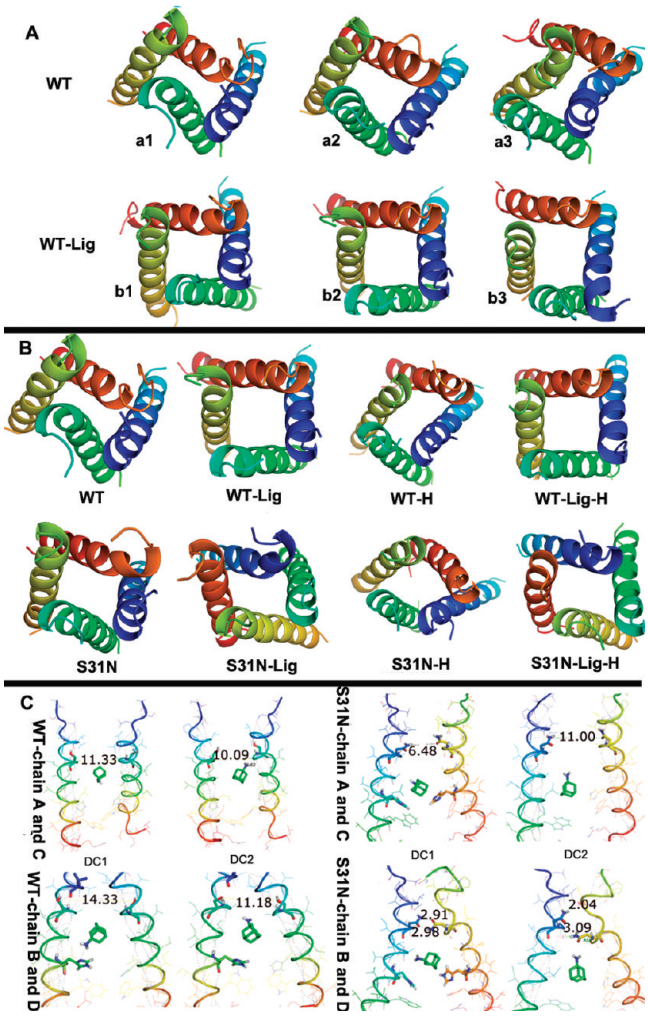

Figure 4. M2 channel motion behavior and steric hindrance M2 channel. (A) M2 channel motion behavior in WT and WT-Lig systems; all three parallel simulations displayed. (B) Average structures of the eight systems (only one of the three parallel simulations is shown in each system). (C) Steric hindrance M2 channel in WT and S31N system in their dominated conformations (DC). DC1 and DC2 represent two dominated conformations in the trajectories.

rmsd of the trajectories of each simulated complex. In further analysis, average conformations in each trajectory were used.

From the independent simulation of WT system, we found that the chains were not moving in the same modes [Figure 4A-a1,a2,a3]. In simulation A1 (A1 is the first simulation trajectory of WT system), chains B and D moved closer, but chains A and C moved farther. In simulation A3, an opposite motion with chains A and C moving closer was observed. As a more average state, the motion in simulation A2 was less asymmetrical. The random movements consistent with other experiments,[25] and are characteristic of the homological tetramer. Interestingly, the asymmetrical motion of M2 channel can be blocked by AMT [Figure 4A-b1,b2,b3]. In all three independent simulations, wild type M2 protein is stable with the binding of AMT and the structure of the tetramer is very symmetrical.

Analyzing all simulation trajectories, we have found that only the protein structures in the WT-Lig and WT-Lig-H systems remain stable and symmetrical [Figure 4B]. Mutation systems, no matter with or without AMT, show obvious heterogeneity in the conformational movement. It indicates that the protein behavior of mutation systems with AMT might be the same as that of WT systems without AMT binding. We speculate that

TABLE 2: Hydrophobic Parameters of Amino Acids in M2 Trans-Membrane Peptides Which Were Reported To Lead to Drug Resistance

	26[a]	27[a]	30[a]	31[a]	34[a]
wild type	L	V	A	S	G
hydrophobic param	3.8	4.2	1.8	−0.8	−0.4
antidrug mutation	F	A	T	N	E
hydrophobic param	2.8	1.8	0.7	−3.5	−3.5

[a] Amino acid identification.

the motions of the protein structures are confined in the WT-Lig and WT-Lig-H systems by the AMT binding to the protein, so there is no obvious heterogeneity in the protein conformational movements. In the WT and WT-H systems, and also in mutation systems with or without ligands, the movements of the chains are not confined and can show heterogeneity as found by experiments.[25]

We analyzed one of the trajectories in WT-Lig and S31N-Lig systems and found the heterogeneity of protein structure movements can be detected in the domain between residues 26 and 35. In the WT system, the distance of each pair of diagonal chains in this domain remains at about 10 Å in the dominant conformations [Figure 4C]. At this normal distance the channel pore in the region between Ser31 and Ala34 is big enough to hold AMT, when it binds the region near Ser31. However, as shown in Figure 4C, when Ser31 was mutated to Asn, the polarity of each chain becomes stronger. Asn31 can interact with another Asn31 from the diagonal chain. This also allows the formation of hydrogen bonds with Ala30 or Val28 from the diagonal chains [Figure 4C]. The distance between the two chains in one diagonal pair in the N-terminal shortens, and the steric hindrance of the channel at position 31 becomes much stronger than that in the WT for AMT binding. This conformational change of M2 chains may play a key role in AMT binding site change.

Hydrophobic Effects and Binding Energy Drives Different Binding Patterns. At the N-terminal part of M2 channel (residues 26−35: LVVAASIIAI), there is only one hydrophilic residue, Ser31. This hydrophobic environment might be essential for M2 function or drug binding. By summarizing other AMT-resistant mutations,[6] it is found that all of them increase the hydrophilic effect in the channel [Table 2]. The most common drug-resisting mutation S31N makes the channel more hydrophilic in the trans-membrane domain. Unfortunately, AMT is well-known as a hydrophobic drug. When the hydrophobic binding environment becomes more hydrophilic, it becomes harder for AMT to enter into the channel and binding.

The calculated QM/MM results also indicate the difference in energy of the interaction between AMT and M2 protein of the WT and S31N mutation. On the one hand, the interaction energy between AMT and M2 protein in WT system is −17.3 kcal/mol when AMT is located between Ser31 and Ala34, while the energy decreases to −7.6 kcal/mol, when S31N mutation system is considered. This energy difference suggests the binding affinity of AMT and M2 protein is sharply decreased in the S31N mutation system, which may contribute to the essential role of binding sites of AMT. On the other hand, when AMT is optimized to the position near His37, the total energy of the S31N-Lig system is 22.9 kcal/mol less than the WT-Lig system. These results indicate that the pore between Ser31 and Ala34 is more favorable for AMT in the WT channel rather than in the S31N channel. The position between Ala34 and His37 provides a more stable binding environment for AMT in

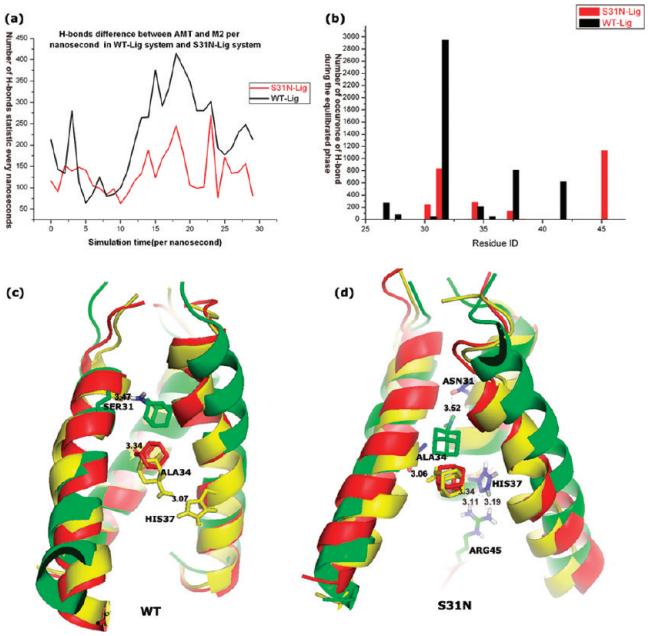

Figure 5. Hydrogen bonds between AMT and M2 channel in the WT-Lig and S31N-Lig systems. (a) Hydrogen bond statistics of WT-Lig and S31N systems per nanosecond during all the 30 ns simulation. (b) Number of occurrence of H-bond formed between AMT and particular residue of WT and mutation M2 protein during the equilibrated phase of the simulation. (c) Snapshots of hydrogen bonds in the WT system. (d) Snapshots of hydrogen bonds in the S31N system.

S31N mutations. The different binding modes can be used to explain why S31N strains are resistant to AMT.

Hydrogen Bonds Stabilize Various Binding Modes. As presented above, the dominant binding site for AMT is located between Ser31 and Ala34 in the WT-Lig system. And for the S31N-Lig system it is near HIS37. To understand the interaction between AMT and M2 protein, hydrogen bonds were analyzed using a tool (g_hbond) in GROMACS.

AMT is more possible to form hydrogen bonds with wild type M2 than the S31N mutation. Figure 5a shows the statistic of H-bond formed every nanosecond. It should be mentioned that, in each snapshot, AMT can only form one hydrogen bond with M2 because AMT has only one polar atom N. In the WT-Lig system, residues 26, 27, 30, 31, 34, 35, 37, and 41 were able to form hydrogen bonds with AMT during 30 ns simulation (not at the same time) [Figure 5b]. Statistical analysis shows that the hydrogen bonds with the highest occurrence frequency are those between AMT and Ser31. At a stable binding site, almost 16.7% the conformations formed hydrogen bonds between AMT and SER31 [Figure 5b].

For the S31N-Lig system, residues 30, 31, 34, 35, 37, 38, 41, and 45 could form hydrogen bonds with AMT [Figure 5b]. When AMT reached a stable binding site, the occurrence of hydrogen bonds between residue 31 and AMT was reduced from 16.7% to 5% [Figure 5b]. Experimental evidence has also shown that Ser31 has some special features. Schnell et al.[10] found that only the amides of Ser31 and Ile32 have NOE cross peaks at the chemical shift of water, which probably corresponds to the exchange of hydroxyl proton of Ser 31 with water. All sequenced variants of M2 have a polar residue in their NMR experiment. The reduction of hydrogen bond formation between AMT and the polar amino acid at position 31 may increase the chemical shift of water, which can be important for the function of the M2 channel. For the S31N mutation system, the dominant hydrogen bonds were formed by Arg45 and AMT. Occurrence frequency of these hydrogen bonds is about 6.7% [Figure 5b]. Arg45 is a flexible residue near the C-terminal end of the transmembrane domain of M2. In our simulation, Arg45 in chain C can get into the hole by forming hydrogen bonds with AMT, and stabilize AMT structure [Figure 5d]. In contrast to the WT-Lig, the hydrogen bonds between Trp41 and AMT have almost disappeared. And the function of M2 protein cannot be disrupted when drug binds to the channel. In all, the different hydrogen bond patterns between the M2 channel and AMT may be one of the key factors for stabilizing AMT at different binding sites and functional variance of the M2 channel.

Functional Analysis Based on a Water Wiring Theory. As far as we know, M2 is a pH-gated proton channel.[9,10] For understanding the proton conductivity in the M2 channel, two mechanisms have been proposed: the gating mechanism and the shuttling mechanism.[26] The gating mechanism suggests that conductivity is achieved by forming a conductive proton wire,[27] where water molecules are able to penetrate the channel throughout. The shuttling mechanism involves histidines.[28] Both of the two mechanisms need water molecules to conduct protons. Water wiring theory has been used to rationalize other MD simulations.[24,26,29−31] In this paper, we choose water wiring theory to explain the proton transportation in the channel.

Influenza A virus M2 protein (A/M2) and influenza B virus BM2 protein are both integral membrane proteins. Both of them are proton-selective channels. However, the only amino acid similarity between the two channels is the HXXXW motif (37−41 in A/M2 and 19−23 in B/M2 respectively). Anti-M2 drug amantadine can only inhibit WT-A/M2 function. Neither B/M2 nor mutated A/M2 channel activity is affected by the drugs. So the difference in the nonconserved domain may play a key role for drug binding in WT-A/M2 and drug resistance in A/M2 mutants or B/M2. In the experiment of replacing residues 6−18 in B/M2 with residues 26−34 from WT A/M2, 50% of the channel activity was inhibited by addition of amantadine.[32] During the simulation, water cannot easily access this domain between residue 26 and 34 in A/M2. Two domains were divided based on water densities: a hydrophobic domain and a hydrophilic domain. The hydrophobic domain ranges from Vlal26 to Ala34, and the hydrophilic one is located at the lower part of the channel. The hydrophobic domain may play a key role in water penetration because it is narrow and hydrophobic for water traveling through. If water cannot get into this domain, the channel might dysfunctional. To confirm this, number of water molecules in the domain of Val27−Ala34 was analyzed. Val27 was chosen instead of Val26 as the terminal position because Val27 is located on the inside face of the pore, forming a second gate in the N-terminal of M2.

For the WT-Lig system, there are few water molecules entering into the channel between Val27 and Ala34 during the simulation. However, when Ser31 was mutated into Asn, water can occupy this region and the average number of water molecules is about 3.3 compared with 1.4 in the WT-Lig system after 10 ns simulation [Figure 6a]. Similarly, there are more water molecules in this region for S31N-Lig-H than in the WT-Lig-H system [Figure 6b]. As a control, both WT and S31N with no ligand were investigated. Water can also occupy this region. The opening of the gate shown in the structure of M2 protein crystallized at low pH makes the channel functional. Two snapshots from WT and S31N are shown in Figure 6c,d. When AMT blocks the entrance of the region near Ser31, water cannot enter into the hydrophobic domain from the lower hydrophilic cavity, thus the water wire will be disrupted and this makes proton transportation defunct. However, in the S31N

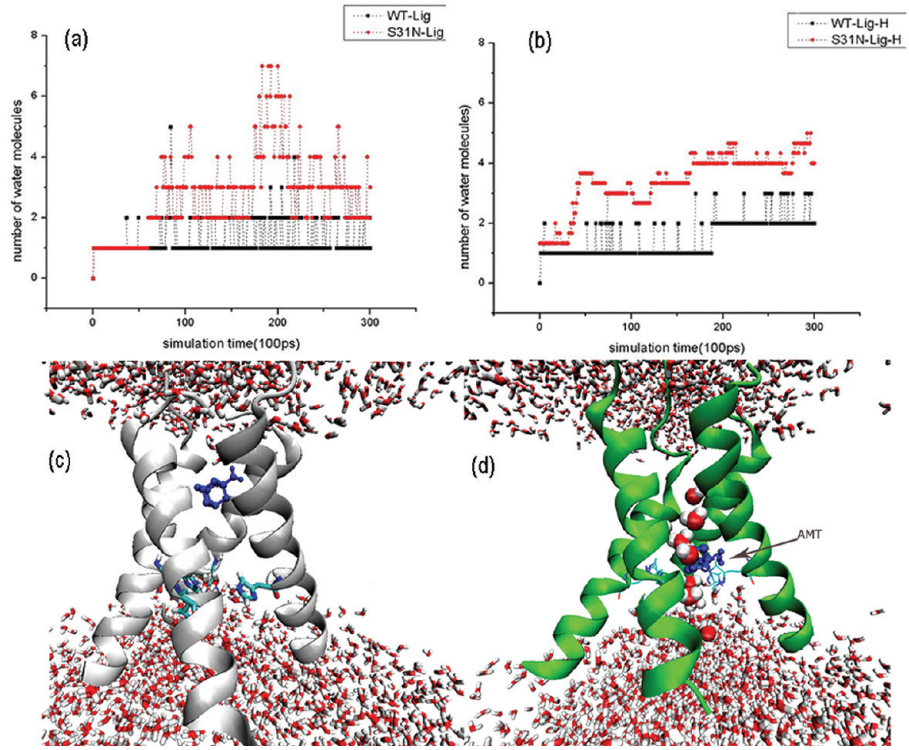

Figure 6. Different binding patterns result in M2 functional difference. (a) Number of waters in hydrophobic domain of M2 (Val26−Ala35) in the WT-Lig and S31N-Lig systems with AMT. (b) Number of water molecules in the hydrophobic domain (Val26−Ala35) of the WT-Lig-H and S31N-Lig-H systems. (c) Snapshots of water molecules in the hydrophobic domain (Val26−Ala35) of M2 in the WT system. (d) Snapshots of water molecules in the hydrophobic domain (Val26−Ala35) of M2 in the S31N system.

system, AMT is located in the hydrophilic domain, and water molecules can enter into the hydrophobic part. The water molecules in this domain can form a water wire which is essential for the proton transfer according to the water wire theory. When AMT fails to block the channel, drug resistance occurs. In other words, S31N mutation can escape from the blocking of AMT as reported based on biological experiments.

Based on the above analysis and discussion, a drug resistant mechanism is proposed. The M2 channel controls water (proton) transportation. Gate residue Trp41 and pH sensor His37 control the entrance of water. Meanwhile, the hydrophobic domain (residue 26−35) plays a crucial role in water transport. When His37 is protonated in a low pH environment, the Trp41 gate open and allows more waters to enter the cavity (hydrophilic domain). The hydrophobic domain allows waters in the cavity to conduct like a wire. When residues in this domain were mutated into more hydrophilic residues, the affinity between water and protein would become stronger, and water conductance would be increased. The motions of the different chains are not the same.

The antivirus drug amantadine can enter into the channel, and block the hydrophobic domain of M2 channel to disrupt the water wire. The hydrophobic residues can form a strong hydrophobic−hydrophobic interaction with AMT, and steric effects allow AMT to stay comfortable in the hydrophobic domain. There is a balance between hydrogen bonds, hydrophobic interaction and steric hindrance. When S31N mutation occurs, the interaction between two pairs of diagonal chains becomes stronger and increases steric hindrance. This also pushes AMT out of the hydrophobic domain. Hydrogen bonds formed between AMT and other residues in the channel can stabilize the new location of AMT, but cannot disrupt the water wire formed in the channel. Therefore AMT becomes inactive in S31N mutations. This mechanism may fit other drug resistant mutations as well.

Conclusions

Our study found a detailed M2 channel behavior and drug resistance mechanism by analyzing the results of molecular dynamics simulations and QM/MM calculations for both WT and the most common drug resistant mutation S31N. The hydrophobic domain (residues 26−35) of M2 channel, which also is the AMT binding site, was found to play a crucial role in M2 function for proton transfer. Amantadine resistance comes from the different binding sites between WT and S31N M2 channel. In the WT system, there is a balance between hydrogen bonds, hydrophobic interaction and steric hindrance when AMT is located between Ser31 and Ala34. When Ser31 was mutated into a more hydrophilic residue Asn, the interaction between two diagonal chains of M2 protein became stronger and led to a stronger steric hindrance. Together with other factors including hydrogen bond interaction patterns, hydrophobic interactions, and binding energy, AMT is stabilized in a new position outside of the hydrophobic domain, resulting in drug resistance.

Our results also support one of the conflicting viewpoints: AMT is effective because it blocks the channel of M2 in the hydrophobic domain. Drug resistance results from a different binding site in M2 channel which does not prevent water (proton) transporting.

Acknowledgment. This work was supported by the State Key Program of Basic Research of China grant 2009CB918502, the Hi-Tech Research and Development Program of China (2006AA01A124, 2009AA01A137), the National S&T Major Project (2009ZX09301-001, 2009ZX09501-001, and 2009ZX09301-001), the Shanghai Committee of Science and Technology grant (08JC1401600) and the National Natural Science Foundation of China grants (20721003, 20720102040, and 20702009). Computation resource was supported by a grant from Information Construction Project of Chinese Academy of Sciences during the 11th Five-Year Plan Period (No.INFO-115-B01).

Supporting Information Available: Rmsd of alpha atoms in the four simulations (Figure S1) and an illustration of the system used in the simulation (Figure S2). This material is available free of charge via the Internet at http://pubs.acs.org.

References and Notes

(1) Kilbourne, E. D. *Emerging Infect. Dis.* **2006**, *12*, 9.
(2) Nayak, D. P.; Hui, E. K.; Barman, S. *Virus Res.* **2004**, *106*, 147.
(3) Russell, R. J.; Haire, L. F.; Stevens, D. J.; Collins, P. J.; Lin, Y. P.; Blackburn, G. M.; Hay, A. J.; Gamblin, S. J.; Skehel, J. J. *Nature* **2006**, *443*, 45.
(4) Pielak, R. M.; Schnell, J. R.; Chou, J. J. *Proc. Natl. Acad. Sci. U.S.A.* **2009**, *106*, 7379.
(5) Yu, K.; Luo, C.; Qin, G.; Xu, Z.; Li, N.; Liu, H.; Shen, X.; Ma, J.; Wang, Q.; Yang, C.; Zhu, W.; Jiang, H. *Cell Res.* **2009**, *19*, 1221.
(6) Suzuki, H.; Saito, R.; Masuda, H.; Oshitani, H.; Sato, M.; Sato, I. *J. Infect. Chemother.* **2003**, *9*, 195.
(7) Cady, S. D.; Hong, M. *Proc. Natl. Acad. Sci. U.S.A.* **2008**, *105*, 1483.
(8) Stouffer, A. L.; Ma, C.; Cristian, L.; Ohigashi, Y.; Lamb, R. A.; Lear, J. D.; Pinto, L. H.; DeGrado, W. F. *Structure* **2008**, *16*, 1069.
(9) Stouffer, A. L.; Acharya, R.; Salom, D.; Levine, A. S.; Di Costanzo, L.; Soto, C. S.; Tereshko, V.; Nanda, V.; Stayrook, S.; DeGrado, W. F. *Nature* **2008**, *451*, 596.
(10) Schnell, J. R.; Chou, J. J. *Nature* **2008**, *451*, 591.
(11) Jing, X.; Ma, C.; Ohigashi, Y.; Oliveira, F. A.; Jardetzky, T. S.; Pinto, L. H.; Lamb, R. A. *Proc. Natl. Acad. Sci. U.S.A.* **2008**, *105*, 10967.
(12) Van Der Spoel, D.; Lindahl, E.; Hess, B.; Groenhof, G.; Mark, A. E.; Berendsen, H. J. *J. Comput. Chem.* **2005**, *26*, 1701.
(13) Siu, S. W.; Vacha, R.; Jungwirth, P.; Bockmann, R. A. *J. Chem. Phys.* **2008**, *128*, 125103.
(14) Schüttelkopf, A. W.; van Aalten, D. M. *Acta Crystallogr., Sect. D: Biol. Crystallogr.* **2004**, *60*, 1355.
(15) Svensson, M.; Humbel, S.; Froese, R. D. J.; Matsubara, T.; Sieber, S.; Morokuma, K. *J. Phys. Chem.* **1996**, *100*, 19357.
(16) Kuno, M.; Hannongbua, S.; Morokuma, K. *Chem. Phys. Lett.* **2003**, *380*, 456.
(17) Svensson, M.; Humbel, S; Morokuma, K. *J. Chem. Phys.* **1996**, *105*, 3654.
(18) Vreven, T.; Mennucci, B.; da Silva, C. O.; Morokuma, K.; Tomasi, J. *J. Chem. Phys.* **2001**, *115*, 62.
(19) Vreven, T; Morokuma, K; Farkas, O; Schlegel, H. B.; Frisch, M. J. *J. Comput. Chem.* **2003**, *24*, 760.
(20) Frisch, M. J.; Trucks, G. W.; Schlegel, H. B.; Scuseria, G. E.; Robb, M. A.; Cheeseman, J. R.; Zakrzewski, V. G.; Montgomery, J. A., Jr.; Stratmann, R. E.; Burant, J. C.; Dapprich, S.; Millam, J. M.; Daniels, A. D.; Kudin, K. N.; Strain, M. C.; Farkas, O.; Tomasi, J.; Barone, V.; Cossi, M.; Cammi, R.; Mennucci, B.; Pomelli, C.; Adamo, C.; Clifford, S.; Ochterski, J.; Petersson, G. A.; Ayala, P. Y.; Cui, Q.; Morokuma, K.; Malick, D. K.; Rabuck, A. D.; Raghavachari, K.; Foresman, J. B.; Cioslowski, J.; Ortiz, J. V.; Baboul, A. G.; Stefanov, B. B.; Liu, G.; Liashenko, A.; Piskorz, P.; Komaromi, I.; Gomperts, R.; Martin, R. L.; Fox, D. J.; Keith, T.; Al-Laham, M. A.; Peng, C. Y.; Nanayakkara, A.; Challacombe, M.; Gill, P. M. W.; Johnson, B.; Chen, W.; Wong, M. W.; Andres, J. L.; Gonzalez, C.; Head-Gordon, M.; Replogle, E. S.; Pople, J. A. *Gaussian 03*, Rev. B.03; Gaussian, Inc.: Pittsburgh, PA, 2003.
(21) Astrahan, P.; Kass, I.; Cooper, M. A.; Arkin, I. T. *Proteins* **2004**, *55*, 251.
(22) Smart, O. S.; Goodfellow, J. M.; Wallace, B. A. *Biophys. J.* **1993**, *65*, 2455.
(23) Intharathep, P.; Laohpongspaisan, C.; Rungrotmongkol, T.; Loisruangsin, A.; Malaisree, M.; Decha, P.; Aruksakunwong, O.; Chuenpennit, K.; Kaiyawet, N.; Sompornpisut, P.; Pianwanit, S.; Hannongbua, S. *J. Mol. Graphics Modell.* **2008**, *27*, 342.
(24) Yi, M.; Cross, T. A.; Zhou, H. X. *J. Phys. Chem. B* **2008**, *112*, 7977.
(25) Yi, M.; Cross, T. A.; Zhou, H. X. *Proc. Natl. Acad. Sci. U.S.A.* **2009**, *106*, 13311.
(26) Kass, I.; Arkin, I. T. *Structure* **2005**, *13*, 1789.
(27) Brewer, M. L.; Schmitt, U. W.; Voth, G. A. *Biophys. J.* **2001**, *80*, 1691.
(28) Lear, J. D. *FEBS Lett.* **2003**, *552*, 17.
(29) Leonov, H.; Arkin, I. T. *J. Mol. Model.* **2009**, *15*, 1317.
(30) Sansom, M. S.; Kerr, I. D.; Smith, G. R.; Son, H. S. *Virology* **1997**, *233*, 163.
(31) Wu, Y.; Voth, G. A. *Biophys. J.* **2005**, *89*, 2402.
(32) Ohigashi, Y.; Ma, C.; Jing, X.; Balannick, V.; Pinto, L. H.; Lamb, R. A. *Proc. Natl. Acad. Sci. U.S.A.* **2009**, *106*, 18775.
(33) Nicholls, A; Bharadwaj, R; Honig, B. GRASP: graphical representation and analysis of surface properties. *Biophys. J.* **1993**, *64*, 166–170.
(34) Faraldo-Gomez, J. D.; Smith, G. R.; Sansom, M. S. P. *Eur. Biophys J.* **2002**, *31*, 217–227.
(35) Kandt, C.; Ash, W. L.; Tieleman, D. P. *Methods* **2007**, *41*, 475–488.

JP911588Y